Indonesian Journal of Electrical Engineering and Computer Science
Vol. 2, No. 2, May 2016, pp. 285 ~ 296
DOI: 10.11591/ijeecs.v2.i2.pp285-296

Model Predictive Current Control of Grid Connected PV Systems

RS Ravi Sankar*, SV Jaya Kumar, KK Deepika
Department of EEE, Vignan's Institute of Information Technology, Visakhapatnam, India, 530046
*Corresponding author, e-mail: satya_ravi2001@yahoo.com

Abstract

This paper deals with the design and simulation of an efficient solar photovoltaic system with a maximum power point tracking system (MPPT). Maximum power point (MPP) is obtained by using Perturb and Observe (P&O) algorithm. The output from solar panel is fed to the DC-DC (Boost) converter which steps up the output voltage. It is then fed to a 3-phase inverter. The inverter used is a 3-phase two-level inverter implemented with a Model Predictive Control strategy. Model of the system is considered in order to predict the control variables. Optimum switching state is selected by minimizing the cost function for each sampling period. This is achieved through modelling and MATLAB simulation of various stages that constitute the overall system.

Keywords*: Model predictive control, three phase voltage source inverter, PV system, Matlab/Simulink*

1. Introduction

Growing interest in integration of renewable energy systems has drawn researchers to explore different VSI control techniques. Photovoltaic (PV) and wind has seen tremendous growth worldwide. PV panels can be used either offline or online. In offline applications, PV panels supply local loads which can be residential or commercial. In online applications, these modules not only supply local loads, but also are connected to the utility grid. In this case, the system would be called "grid-connected PV system. Recently, grid-connected PV system installation is increasing tremendously in many countries. Since the output of PV panels are direct current (in the case of grid-connected PV systems), the interface is typically a DC-AC converter (inverter) which inverts the DC output current that comes from the PV arrays into a synchronized sinusoidal waveform.In general, PV Three phase inverter (TPI) comes with DC-DC converter (normally, a version of Boost), maximum power point tracking (MPPT) control and voltage source inverter (VSI) packed as a single unit.

A Boost converter is a power electronic converter that gives output voltage greater than input voltage of the PV panel. This voltage regulation is attained by PWM. MPPT is achieved by adjusting the duty cycle by using Perturb and Observe method.

2. Research Method

Single phase inverters (usually few kW) with a control in synchronous reference frame have been discussed in [10], and those with model predictive control (MPC) have been reported by [11]. Among all the control techniques model predictive control (MPC) is one of the most popular control approaches because it's simple to implement and has extremely fast dynamic response, it has robust stability characteristics. Conventional switching-table-based MPC is simple, robust, and exhibits excellent transient response. Thus, it is widely used.

MPC considers a model of the system in order to predict behavior of the system in future. A cost function is evaluated to choose the optimal switching states. This paper presents a simple and easy-to-implement approach of modeling MPC based on TPI for grid tied PV systems.

Received December 23, 2015; Revised April 11, 2016; Accepted April 28, 2016

2.1. Mathematical Modeling of PV panel

A PV system consists of a number of PV modules connected in series or parallel to create a DC PV array. Figure 1 illustrates a simple equivalent circuit diagram of a PV cell. PV cell is a simple P-N junction diode which converts solar energy into electrical energy. I_{pv} is the current generated by the light. D1 and D2 are two anti-parallel diodes, R_p is the shunt resistance and R_s is the series resistance. V and I are the voltage and current generated by the PV cell respectively. The implicit V-I relationship is given by:

$$I = I_{pv} - I_{D1} - I_{D2} - \left(\frac{V + IR_s}{R_p} \right) \quad (1)$$

$$I_{D_1} = I_{o1} \left[\exp\left(\frac{q(V + IR_S)}{A_1 KT} \right) - 1 \right] \quad (2)$$

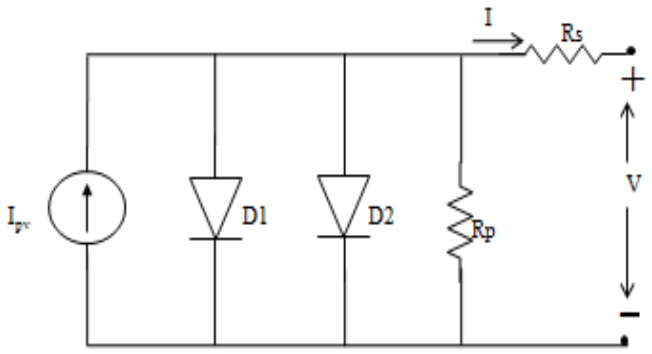

Figure 1. Two diode model of PV cell

$$I_{D_2} = I_{o2} \left[\exp\left(\frac{q(V + IR_S)}{A_2 KT} \right) - 1 \right] \quad (3)$$

$$I_{pv} = \left[I_{scr} + K_i (T_k - T_{refk}) \right] \times \lambda / 1000 \quad (4)$$

Here λ is the solar irradiation, I_{scr} is the PV device short- circuit current, T_k and T_{refk} are, respectively, the actual and reference temperature. $K_i$is the short-circuit current/ temperature coefficient (A/ K), A_1 and A2 are the diode ideality factors. q is the charge of the electron and I_{o1} and I_{o2} are the reverse saturation currents of D_1 and D_2respectively.
Equation (1) is modified for PV module as:

$$I = N_p I_{pv} - N_p I_{D1} - N_p I_{D2} - \left(\frac{V + IR_s}{R_p} \right) \quad (5)$$

$$I = N_p \times I_{pv} - N_p \times I_{o1} \left[\exp\left\{ \frac{q \times (V + IR_s)}{N_s A_1 kT} \right\} - 1 \right] - N_p \times I_{o2} \left[\exp\left\{ \frac{q \times (V + IR_s)}{N_s A_2 kT} \right\} - 1 \right] - \left(\frac{V + IR_s}{R_p} \right) \quad (6)$$

Here N_s and N_p are the No. of cells in series and parallel respectively. The modules are configured in a No.of series and parallel structures with any number of PV modules to produce a PV array.

Now the PV array V-I relationship is given by the following equations.

$$I = N_{pp} \times I_{pv} - N_{pp} \times I_{o1}\left[\exp\left\{\frac{q \times \left(V + IR_s\left(\frac{N_{ss}}{N_{pp}}\right)\right)}{N_{ss} A_1 kT}\right\} - 1\right] - N_{pp} \times I_{o2}\left[\exp\left\{\frac{q \times \left(V + IR_s\left(\frac{N_{ss}}{N_{pp}}\right)\right)}{N_{ss} A_2 kT}\right\} - 1\right] - \left(\frac{V + IR_s\left(\frac{N_{ss}}{N_{pp}}\right)}{R_p\left(\frac{N_{ss}}{N_{pp}}\right)}\right) \quad (7)$$

Here N_{ss} and N_{pp} are the number of modules connected in series and parallel, respectively. In this paper, standard KC200GT datasheet parameters are used to implement the PV system in a SIMULINK environment.

Table 1. KC200GT parameter specifications

Maximum Voltage (V_m)	26.3V
Current at Maximum Power (I_m)	7.61A
Open Circuit Voltage (V_{oc})	32.9V
Short Circuit Current (I_{sc})	8.21A
Total No.of Cells in Series (Ns	54
Total No.of Cells in Parallel (N_p)	1
Temperature Coefficient of V_{oc}(K_v)	-123 mV/^{o}C
Temperature Coefficient of I_{sc}(K_i)	3.18mA/^{o}C
saturation current I_{o1} = I_{o2}	1.045×10−^{9}A
R_p	415.405 Ω.
R_s	0.221

By using the above KC200GT parameters a PV system is designed using MATLAB/SIMULINK environment. The maximum power point tracking system is used to extract maximum power from the PV panel. The problem considered by MPPT techniques is to automatically find the voltage or current at which a PV array should operate to obtain the maximum power output under a given temperature and irradiance. This ensures that the panel delivers maximum power to the system. Among the different methods used to track the maximum power point, Perturb and Observe method is the most widely used method in PV MPPTs and is highly competitive against other MPPT methods.

2.2. Perturb and Observe Method

In Perturb and observe (P&O) method, the MPPT algorithm is based on the calculation of the power of the PV panel and change in power, by sampling both the PV current and voltage. The tracker operates by periodically incrementing or decrementing the solar array voltage. This algorithm is summarized in table 2.

Table 2. Summary of P&O algorithm

Change in voltage	Change in power	Next pertubation In duty cycle
Positive	Positive	Increased
Positive	Negative	Decreased
Negative	Positive	Decreased
Negative	Negative	Increased

At MPP, rate of change of power is zero. In next sampling instant, power extracted decreases and hence the perturbation reverses as shown in Figure 2. In this method the stable condition is arrived around the peak power point. In order to maintain the power variation small the perturbation size is remain very small.

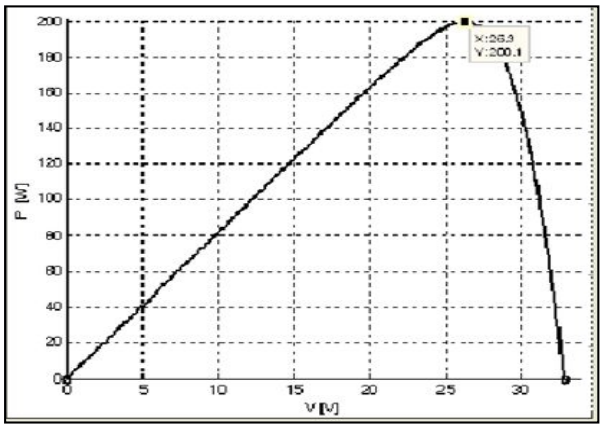

Figure 2. PV panel characteristics

The algorithm involves perturbations on the duty cycle of the DC-DC power converter *(D)*, Voltage of the DC-link that is between the PV array and the power converter *(V)*.

If *P(k)> P(k-1),* then the direction of perturbation on duty cycle is maintained. And if $\Delta V < 0$, the voltage is increased by increasing the duty cycle as $D(k)= D(k-1)+C$ where C is step size else if $\Delta V > 0$, the voltage is decreased by increasing the duty cycle as $D(k)= D(k-1)- C$.

If *P(k)< P(k-1),* then the direction of perturbation is reversed. This is explained in Figure 3.

2.3. DC-DC Boost Converter

A Boost converter is a power electronic converter that gives output voltage greater than input voltage. When both the input and the output quantities are DC voltages, it is known as a DC-DC boost converter or step-up converter. Figure 4 illustrates a type of boost converter which consists of one controlled switch, S (IGBT), one uncontrolled switch (diode), D and two energy storage devices like inductor and capacitor.

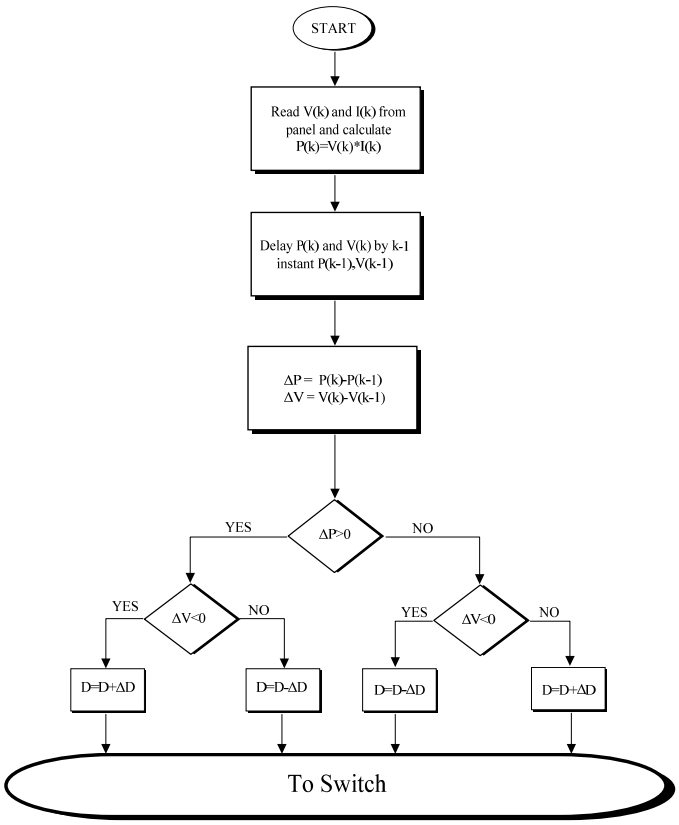

Figure 3. Flow Chart for P&O algorithm

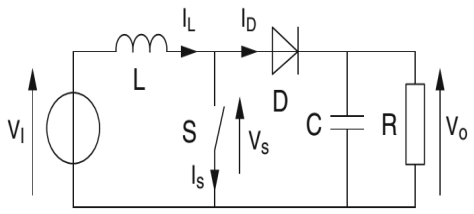

Figure 4. Boost converter circuit

Gate signal from MPPT controller is given to the converter and values of L, C are designed by using design equations. Values of L, C are varied to get the required output voltage. The input voltage to the dc-dc boost converter is V_s = 152V and the output voltage of dc-dc boost converter is V_{dc} = 300V. The capacitance C=15mF and inductance L=0.1mH.

2.4. Three-Phase Grid-Connected Inverters

Figure 5 shows a three phase bridge inverter which consists of six controlled switches (IGBT). To maintain constant DC input capacitor filter is connected between the PV and inverter circuit. Terminals A, B, C are connected to three phase load or to the grid.

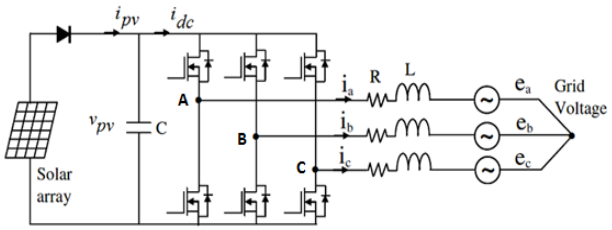

Figure 5. Three-phase grid-connected scheme

The input dc in Figure 5.1 is obtained from a solar array. The switching states of the converter are determined as follows:

$$S_a = \begin{matrix} 1, & \text{if } S_1 \text{ is on and } S_4 \text{ is off} \\ 0, & \text{if } S_1 \text{ is off and } S_4 \text{ is on} \end{matrix} \quad (7)$$

$$S_b = \begin{matrix} 1, & \text{if } S_2 \text{ is on and } S_5 \text{ is off} \\ 0, & \text{if } S_2 \text{ is off and } S_5 \text{ is on} \end{matrix} \quad (8)$$

$$S_c = \begin{matrix} 1, & \text{if } S_3 \text{ is on and } S_6 \text{ is off} \\ 0, & \text{if } S_3 \text{ is off and } S_6 \text{ is on} \end{matrix} \quad (9)$$

Where gating signals S_a, S_b, and S_c And can be expressed in phasor form by

$$S = \frac{2}{3}\left(S_a + aS_b + a^2 S_c\right) \quad (10)$$

Where, $a = e^{j\left(2\pi/3\right)}$,
The output-voltage space vectors generated by the inverter are defined by

$$V_i = \frac{2}{3}\left(V_{aN} + aV_{bN} + a^2 V_{cN}\right) \quad (11)$$

where V_{aN}, V_{bN} , and V_{cN} are the phase voltages of the inverter, with respect to the negative terminal of the dc link N.

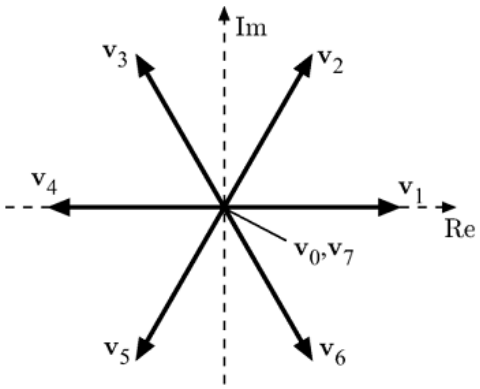

Figure 6. Possible voltage vectors generated by the inverter

Then, the load voltage vector $\mathbf{V_i}$ can be related to the switching state vector **S** by

$$V_i = V_{dc} S \tag{12}$$

Where V_{dc} is the dc-link voltage. Considering all the possible combinations of the gating signals S_a, S_b, and S_c, eight switching states and, consequently, eight voltage vectors are obtained, as shown in Table 4, using (12). Here, variables S_a, S_b, and S_c represent the switching states of the a, b, and c legs of the inverter. Note that $V_0 = V_7$.

Table 4. Switching sequence of three phase inverter

Switching states			Output voltage
S_a	S_b	S_c	V_i
0	0	0	$V_0 = 0$
1	0	0	$V_1 = \frac{2}{3}V_{dc}$
1	1	0	$V_2 = \frac{V_{dc}}{3} + j\frac{\sqrt{3}}{3}V_{dc}$
0	1	0	$V_3 = \frac{V_{dc}}{3} + j\frac{\sqrt{3}}{3}V_{dc}$
0	1	1	$V_4 = \frac{-2V_{dc}}{3}$
0	0	1	$V_5 = \frac{V_{dc}}{3} - j\frac{\sqrt{3}}{3}V_{dc}$
1	0	1	$V_6 = \frac{V_{dc}}{3} - j\frac{\sqrt{3}}{3}V_{dc}$
1	1	1	$V_7 = 0$

2.5. Model Predictive Control

The proposed strategy predicts the behavior of the variables for each switching state. These states are discrete and a discrete-time model of the system is used to predict the behavior of VSI system. An objective function is defined to minimize the error between the output currents and reference currents, by choosing the optimum switching state for each sampling period.

MPC is implemented in αβ reference frame with 6 nonzero voltage vectors and 2 zero voltage vectors. In addition, load dynamics are modeled as:

$$v = L\frac{di}{dt} + Ri + \mathrm{e} \tag{13}$$

Where R L and *e*are load resistance, inductance and back emf respectively, i is the load current and $\boldsymbol{v}$ is the VSI generated voltage vector.
Using Euler-Forward equation, the load current is approximated by:

$$\frac{di}{dt} \cong \frac{i(k+1) - i(k)}{T} \tag{14}$$

Using (13) and (14), we can approximate

$$i^p(k+1) = \left(1 - \frac{RT}{L}\right) i(k) + \frac{T}{L} v(k) - e(k) \tag{15}$$

Where k=t (present) and k+1=t+1(future/predicted) value.

In each switching state, load current is estimated using Equation (15). The objective function is evaluated to calculate the optimal value of the load current, for every switching state. The optimal load current is applied during the next sampling period. VSI MPC control system is illustrated in Figure. 7.

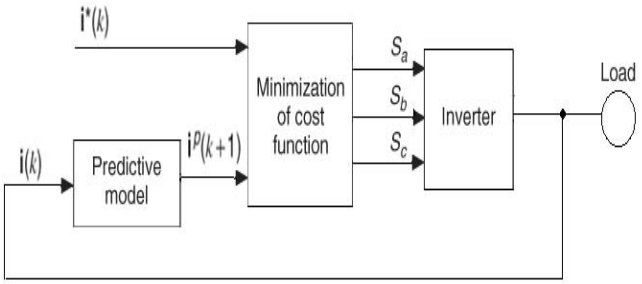

Figure 7. VSI MPC control block diagram

All the variables are initialized. Using from (13), the back-emf can be calculated as :

$$e(k-1) = v(k-1) - \frac{L}{T} i(k) - \left(R - \frac{L}{T}\right) i(k-1) \tag{16}$$

The back-emf e(k), neded in (15), is estimated using an extrapolation of its past values. Figure 8 outlines step by step implementation process of Model Predictive Control of VSI. The objective function here is given by the equation:

$$g = \left|i_\alpha^* - i_\alpha^p\right| + \left|i_\beta^* - i_\beta^p\right| \tag{17}$$

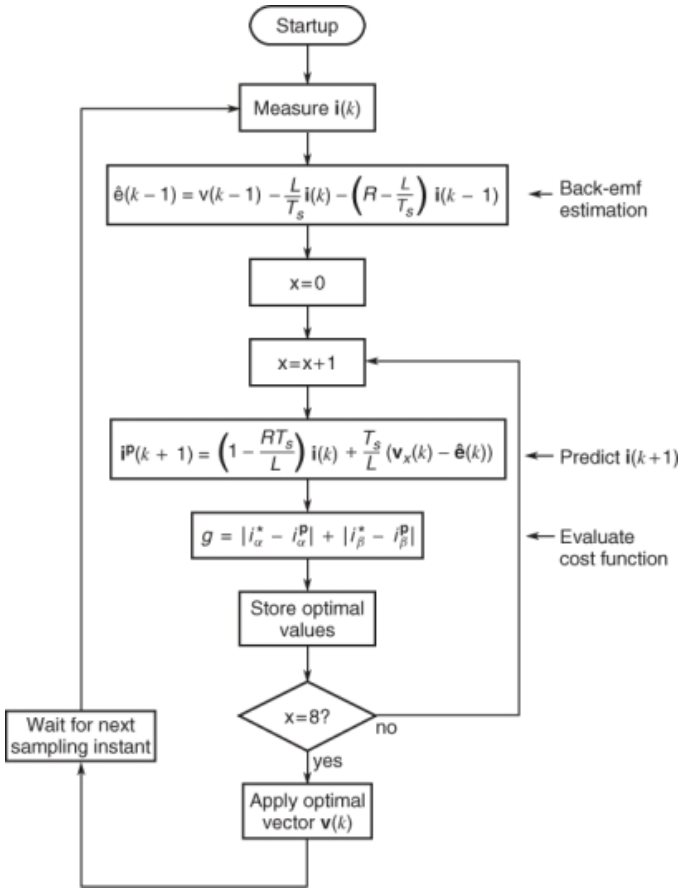

Figure 8. Flow chart for MPC control of VSI

Objective function, *g* given by (17) is used to minimize the error between the estimated output and reference current and the optimal *g*(k+1) is selected for switching state is applied across VSI in the next sampling period. Note that in each sampling period 8 predictions are made and 8 objective functions are evaluated before selecting the control action, S(k) for the next sampling period.

3. Results and Analysis

Simulations of a three phase voltage inverter with RL load were carried out using MATLAB/SIMULINK and the model is shown in Figure 9.

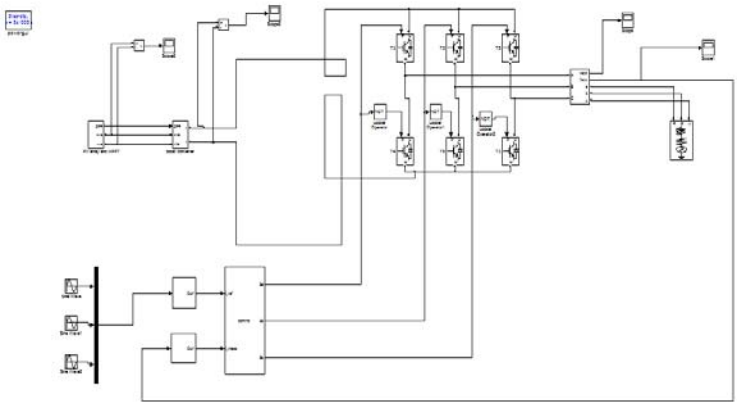

Figure 9. Simulink model of MPCC VSI

Table 5. Simulink Parameters

Parameters	Values
Supply voltage	300V
Resistance	0.36ohm
Inductance	4.7mh
Sampling time	50e-6
Reference Current	10A

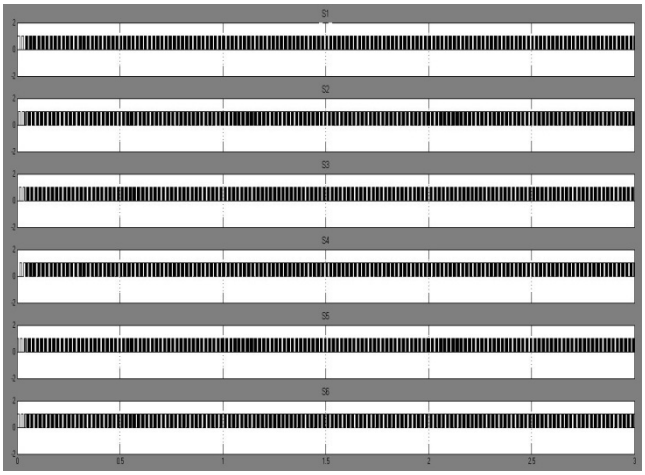

Figure 10. Switching statesof grid connected inverter

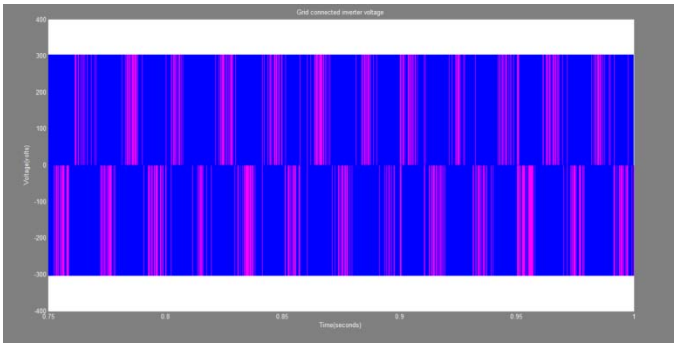

Figure 11. Three phase voltage of grid connected inverter

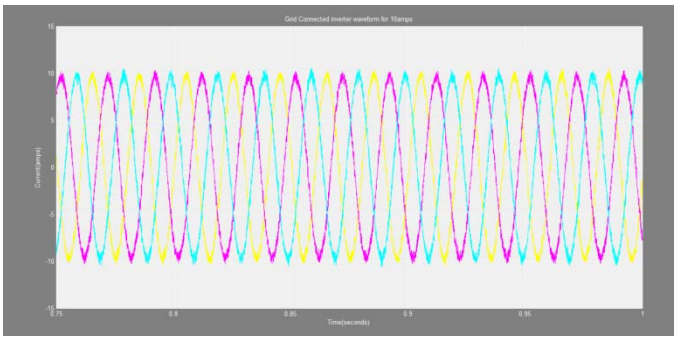

Figure 12. The grid connected inverter current waveform for 10amps

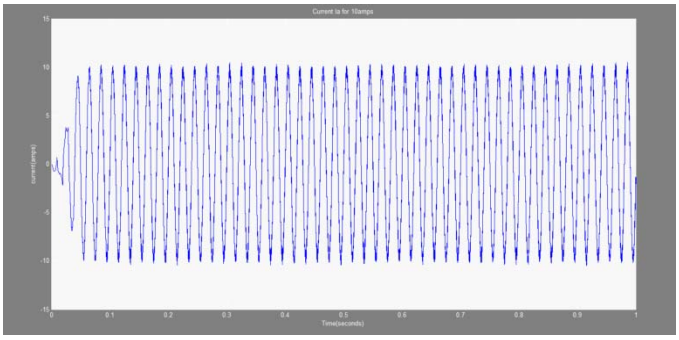

Figure 13. Current $\mathbf{I}_{\alpha}$ for 10amps

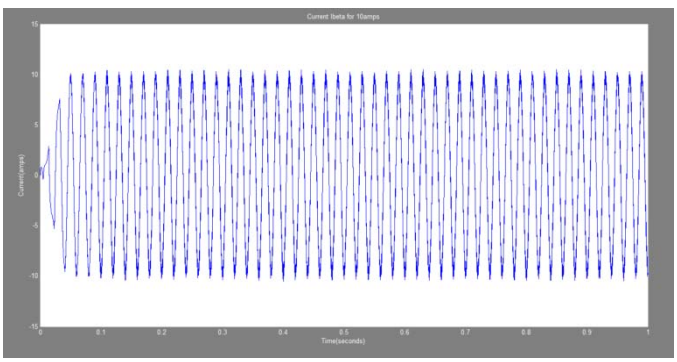

Figure 14. Current $\mathbf{I}_{\beta}$ for 10 amps

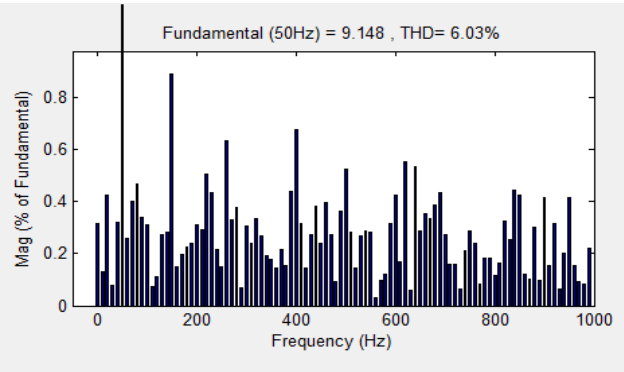

Figure 15. Total Harmonic Distortion for 10amps

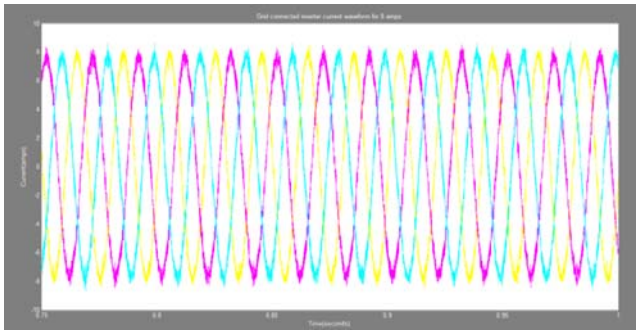

Figure 16. Grid connected inverter current waveform for 8amps

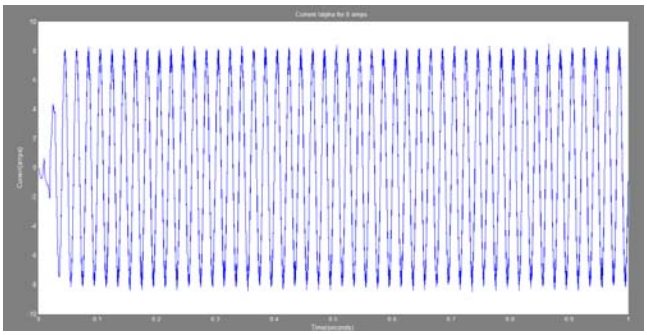

Figure 17. Current $\mathbf{I}_{\alpha}$ for 8amps

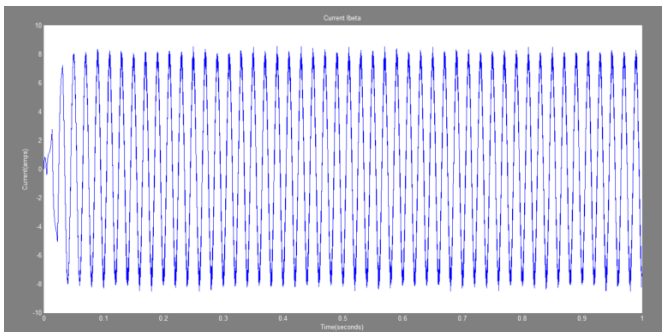

Figure 18. Current $\mathbf{I}_{\beta}$ for 8amps

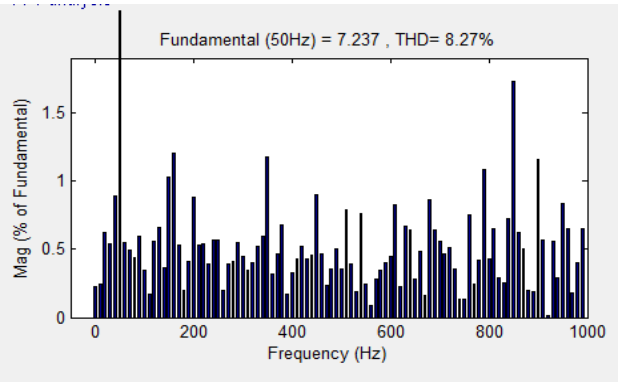

Figure19. Total Harmonic Distortion for 8amps

Table 6. THD for various Reference currents

Reference Current(amps)	Fundamental Frequency (50Hz)	Total Harmonic Distortion (%)
10	9.148	6.03
8	7.237	8.27
6	5.099	12.90
4	3.132	18.61
2	1.037	70.41

4. Conclusion

This paper presented MPC of a TPI for a PV system. The MPC based TPI model resulted in a simpler control and implementation without sacrificing quality and accuracy. The poor performance and saturation of conventional PWM and PI regulators can be avoided by MPC. The adequacy of the MPC model in tracking the reference was validated in Matlab/Simulink.

References

[1] SB Kjaer, JK Pedersen and F Blaabjerg. “A review of single-phase grid-connected inverters for photovoltaic modules”. *IEEE Trans. Ind. Appl*. 2005; 41(5): 1292–1306.
[2] J Rodrguez, J Pontt, CA Silva, P Correa, P Corts and U Ammann. “Predictive Current Control of a Voltage Source Inverter”. *IEEE Trans. Ind. Electron*. 2007; 54(1): 495–503.
[3] J Nedumgatt, K Jayakrishnan, S Umashankar, D Vijay acumen and D Kothari. “*Perturb and observe MPPT algorithm for solar PV systems-modeling and simulation*”. Proceedings of Annual IEEE India Conference (INDICON). 2011; 1–6.
[4] SB Kjaer, JK Pedersen and F Blaabjerg. “A review of single-phase grid-connected inverters for photovoltaic modules”. *IEEE Trans. Ind. Appl*. 2005; 41(5): 1292–1306.
[5] P Cortés, MP Kazmierkowski, RM Kennel, DE Quevedo and J Rodríguez. “Predictive control in power electronics and drives”. *IEEE Transactions on Industrial Electronics*. 2008; 55(12): 4312–4324.
[6] J Holtz and S Stadtfeld. “A predictive controller for the stator current vector of AC machines fed from a switched voltage source”. in *International Power Electronics Conference, IPEC*, Tokyo. 1983: 1665–1675.
[7] O Kukrer. “Discrete-time current control of voltage-fed three-phase PWM inverters”. *IEEE Transactions on Industrial Electronics*. 1996; 11(2): 260–269.
[8] J Hu, J Zhu, G Lei, G Platt and DG Dorrell. “Multi-objective model-predictive control for high power converters”. *IEEE Trans. Energy Convers*. 2013; 28(3): 652–663.
[9] S Buso and P Mattavelli. “Digital Control in Power Electronics”. ser. 978-1598291124. Denver: Morgan and Claypool Publishers. 2006.
[10] M Monfared, S Golestan and JM Guerrero. "Analysis, Design, and Experimental Verification of a Synchronous Reference Frame Voltage Control for Single-Phase Inverters". *IEEE Trans. Ind. Electron*. 2014; 61(1).
[11] IM Syed and K Raahemifar. “Model Predictive Control of Single Phase Inverter for PV System”. *Intl. J. of Elec. Comp. Electro. And Comm. Eng*. 2014; 8(11).